We are IntechOpen, the world's leading publisher of Open Access books Built by scientists, for scientists

4,800
Open access books available

122,000
International authors and editors

135M
Downloads

Our authors are among the

154
Countries delivered to

TOP 1%
most cited scientists

12.2%
Contributors from top 500 universities

CLARIVATE ANALYTICS BOOK CITATION INDEX INDEXED

WEB OF SCIENCE™

Selection of our books indexed in the Book Citation Index in Web of Science™ Core Collection (BKCI)

Interested in publishing with us?
Contact book.department@intechopen.com

Numbers displayed above are based on latest data collected.
For more information visit www.intechopen.com

3

Application of Orientation Mapping in TEM and SEM for Study of Microstructural Evolution During Annealing – Example: Aluminum Alloy with Bimodal Particle Distribution

K. Sztwiertnia, M. Bieda and A. Kornewa
Polish Academy of Sciences, Institute of Metallurgy and Materials Science, Krakow, Poland

1. Introduction

There are still considerable gaps in the understanding of the recrystallization processes of metallic materials, which reduce the possibility of controlling their course and introducing technological modifications aimed at obtaining desirable properties. The lack of a complete explanation can be attributed to the high complexity of the phenomenon, which consists of a superposition of the local nucleation and grain growth processes. These processes depend strongly on the characteristics of the matrix, which is typically complex and heterogeneously deformed. The phenomenology of the process and its energetic causes are known because they were examined long ago, e.g., (Humphreys & Hatherly, 2002). On the other hand, the relevant physical mechanisms that control the nucleation and growth of new grains are not entirely clear. This uncertainty exists, among other reasons, because the origin of the crystallographic orientations of the nuclei is usually not known.

1.1 Crystallographic orientation and orientation characteristics of materials

The crystallographic orientation is a feature of a material that is defined at any point of the sample at which the ordering of the crystal lattice is not disturbed (or not significantly disturbed). It can be generally said that almost all of the basic quantities that characterize a polycrystalline material and its properties have a direct or complex relationship to the orientation (g_i), which is a function of the coordinates x_i, y_i, z_i of a point in the sample. The $g(x,y)$ function described in a plane of the sample defines the orientation topography (commonly called the orientation map). According to the definition of the term, the orientation at any point (x_i, y_i) in the sample is given by a rotation that brings the local sample reference system with its origin at the point (x_i, y_i) into coincidence with the crystal reference system. The orientation is described unambiguously by three parameters, which can be expressed in different ways. Usually, for the convenience of calculation, the Euler angles φ_1, Φ, φ_2 are applied. In some cases, the parameters of the rotation axis (θ, ψ) and the rotation angle ω are used because this scheme is easy to visualize. If the orientation is described by a greater number of parameters, then the parameters depend on each other.

Such is the situation in the case of crystallographic indices {hkl}<uvw>, commonly used in practice. Extensive analysis of orientation problems can be found in (Morawiec, 2004). If an orientation map is obtained, the grains or subgrains may be reconstructed by identifying areas whose pixels have orientations within a specified range. The knowledge of the orientation topography enables the identification of grain and subgrain boundaries, as well as other microstructural inhomogeneities, by selection of misorientations between neighboring measuring points. This approach enables stereological analysis with regard to the crystallographic orientation. Based on the orientation topography, the orientation characteristics of the microstructure can be determined (Pospiech et al., 1993). The set of orientation characteristics comprises the "principal distributions", which are texture functions determined by the whole set of measurements and "partial distributions", in which only part of measurements are needed. The most important of the principal distributions is the well-known orientation distribution function (ODF), which describes the crystallographic texture of a material. The ODF is defined by the density of the global orientation distribution of the grains (taking into account their volume fraction). Another "principal distribution" is the orientation difference distribution function (ODDF). The ODDF contains all possible misorientations between the measured orientations. To investigate local textures (or microtextures) in selected areas of inhomogeneities or in the environment of preferred orientations, partial distribution functions are applied. The most important of these functions is the misorientation distribution function (MODF), which describes the distribution of misorientation between the nearest neighbor grains. The other partial orientation distributions are statistical quantities related to orientation and misorientation, which may be related to the properties of a material, its anisotropy or specific stages through which material passes (Pospiech et al., 1993).

Many of the essential properties of polycrystalline materials and their anisotropy depend directly or indirectly on the topographical arrangement of orientations. Using the orientation topography, the material properties that depend on the character and distribution of the grain boundaries can be described, for example, segregation or corrosion. The knowledge of the orientation topography is of basic importance for the understanding of many processes that occur in the material, such as deformation, recrystallization, phase transformation or diffusion.

It is, therefore, not surprising that the characterization of the microstructure based on the sets of measured orientations has advanced as a well-established technique, known as Orientation Microscopy (OM). The main concept behind this technique is the automatic collection and indexing of many electron diffraction patterns that are correlated with sample coordinates. The development of new generations of computer-controlled electron microscopes has improved their spatial resolution and increased the rate at which large sets of Electron Back Scattered Diffraction (EBSD) patterns can be collected and processed in a Scanning Electron Microscope (SEM), e.g., (Dingley, 1984; Wright & Adams, 1992; Adams & Dingley, 1994; Schwartz et al., 2009). Systems created orientation topographies using EBSD in SEM are now very common, and commercially available versions of this technology are essentially fully automated, e.g., (HKL, 2007; TSL, 2007).

1.2 Orientation imaging microscopy for recrystallization study

Obviously, the analysis and modeling of the recrystallization of a deformed metallic material requires description of the microstructure evolution during annealing that is as

complete as possible. Such a description may be based on the orientation topographies obtained by OM techniques in systematic measurements of a sample that undergoes a specific deformation and annealing process, e.g., (Zaefferer et al., 2001; Sztwiertnia, 2008).

To study the recrystallization (particularly its early stages), a high spatial resolution in the orientation measurement is required. Unfortunately, the spatial resolution that can be achieved by EBSD/SEM measurements is relatively low. It falls approximately one order of magnitude behind the spatial resolution in conventional SEM imaging, and still further behind when compared to the spatial resolution of a transmission electron microscope (TEM). The measurement is limited in this way because the inherent resolution of EBSD is governed not by the diameter of the beam spot at the point of impact on the surface, but primarily by the excitation volume. This quantity is the fraction of the interaction volume of the primary electrons within the sample from which the pattern-forming electrons are back diffracted and leave the crystal, without further scattering. This volume is strongly dependent on the type of electron gun and the material being investigated. Tilting of the sample during the EBSD measurement further degrades the spatial resolution and produces resolution along the beam direction on the sample surface that is approximately three times worse than the resolution along the direction perpendicular to the beam, e.g., (Schwartz et al., 2009). For these reasons, the best achievable spatial resolution in EBSD/SEM special cases is in the order of approximately 30 nm; however, the practical limit is approximately 100 nm. This limitation restricts the utility of EBSD/SEM for the investigation of very fine-grained and deformed microstructures, as in the case of the early stages of recrystallization. To obtain better spatial and angular resolution, similar systems have been developed for TEM, e.g., (Haessner et al., 1983; Dingley, 2006; Morawiec, 1999; Morawiec et al., 2002; Rauch & Dupuy, 2005). Despite some restrictions, such as the currently unsolved problems of image analysis, difficulties in measurement automation and sample preparation, the OIM technique applied to TEM offers spatial resolution better than 10 nm and can be used for quantitative analysis of structures at the nanoscale. Such a system, built at the Institute of Metallurgy and Materials Science (Morawiec et al., 2002; Sztwiertnia et al., 2006; Bieda-Niemiec, 2007), was used for a study of the recrystallization of 6013 aluminum alloy (Sztwiertnia et al., 2007; Bieda et al., 2010).

The 6013 aluminum alloy was chosen as a prototype material that represents a group of commercial alloys with a bimodal second phase particle distribution. The second-phase particles are used to control the strengthening, grain size and texture of the alloy. Such alloys can be interesting for examination of the role of the second phase particles in the recrystallization process, e.g., (Humphreys & Hatherly, 2002; Sztwiertnia et al., 2005; Ardakani & Humphreys, 1994).

To elucidate the mechanisms of the alloy microstructure transformation during annealing, *in situ* TEM experiments and combined calorimetric–microscopic investigations of bulk samples were carried out. The *in situ* experiments were necessary to provide information about the temporal relationships between changes that occur in the metal at the beginning of recrystallization. Dynamic studies using SEM or TEM should be capable of providing the required information. Because of its already mentioned limitations, the EBSD/SEM measurements of localized strain in the deformed polycrystal, which are particularly interesting as nucleation sites, give rather poor information about the orientation. For the *in situ* studies of such regions, measurements using convergent beam electron diffraction

(CBED) or microdiffraction in a TEM are more suitable, although the proximity of the free surface in the thin foils can be a complicating factor during annealing. The first *in-situ* TEM observations, obtained by Bailey in 1960 and Hu in 1963, indicated differences in the recrystallization processes that can occur during the annealing of bulk samples and thin foils. As a consequence, many researchers have been skeptical about the results of such experiments up to now. However, the results obtained later by other authors e.g., (Roberts & Lehtinen, 1972; Hutchinson & Ray, 1973; Sztwiertnia & Haessner, 1994) allow the determination of the experimental conditions, which ensures that the changes directly observed in an annealed foil are at least similar to those occurring in a bulk sample. In general, recrystallization is easiest in orthogonal sections from a rolled sheet in which the grain boundaries, extending from top to bottom of the foil, present the most favorable distribution of driving potential for migration. Grooving grains are not strongly inhibited in the thin foil regions and frequently extend nearly to the edge of the foil (Hutchinson & Ray, 1973). Nevertheless, because of the thermal grooving, the recrystallization front always stops in foil thinner than a certain critical value, which approximately depends on the fineness of its microstructure. One can increase the usable foil thickness by increasing the accelerating voltage. The impact of the sample thickness on grain boundary movement explained in greater detail by Roberts & Lethinen, 1972.

In highly deformed 6013 aluminum alloy, the critical thickness for foils cut from planes perpendicular to the sheet is so low that it allows *in situ* observation of nucleation events (and to some extend the growth of the nuclei) to be carried out in a conventional TEM operated at 200 kV (Sztwiertnia et al., 2005; Sztwiertnia et al., 2007; Bieda et al., 2010). To examine the significance of the *in situ* experiments, the thin foils annealed in the TEM were compared to thin foils prepared from bulk samples heated in a calorimeter to obtain a specified recrystallization stage. The comparison shows that the processes occurring in both types of foils were at least qualitatively the same.

2. Example: Recrystallization of aluminum alloy with bimodal particle distribution

2.1 Material and investigation methodology

The changes of the microstructure during annealing were examined in the case of the polycrystalline aluminum alloy 6013 (Table 1), which was previously identified as the prototype of materials with a bimodal precipitate distribution.

Mg	Si	Cu	Mn	Fe	others	Al
1.15	1.0	1.1	0.3	0.5	0.15	remainder

Table 1. 6013 aluminum alloy chemical composition (% wt.).

Samples for testing were supersaturated, then aged and reversibly cold-rolled up to the 75 and 90 % of the 10 mm value. The deformed samples were examined by means of non-isothermal annealing in a differential calorimeter (DC). It was found that the spectrum of released stored energy contained several peaks. Next, a new series of samples were heated in the calorimeter to the selected temperatures, rapidly cooled, and then analyzed in the TEM. The tests in the TEM were complemented by SEM examinations. Because of the poor quality of the orientation

topographies measured by the standard EBSD/FEG/SEM techniques, these measurements were used only to detect the presence of newly recrystallized grains (that is, only those diffraction patterns were taken into account that had a high image quality and showed local areas with low dislocation densities). The high degree of deformation also resulted in low quality TEM diffraction patterns. However, it was still possible to measure enough single orientations in the TEM to construct orientation topographies for all of the microstructural elements of the cold-rolled material. The investigations also included a comparison of the deformed alloy microstructure with that of the pure metal and the investigation of the recrystallization process dynamic. The latter investigation consisted of the *in situ* measurements in the TEM. This measurement was necessary to obtain information about the time sequence of changes occurring in the material at the beginning of the recrystallization. In the investigated material, the sequence of events that occurs in the deformation zones is of particular interest because such areas undergo intense nucleation.

2.2 Deformation state

First, the deformation microstructure of the alloy was compared with that of the pure metal. The microstructure of commercially available pure aluminum (3N Al), reversibly cold rolled to 90%, has been chosen for comparison. Both microstructures are built of elongated in the rolling direction (RD) and lie nearly parallel to the sheet plane grains and subgrains, as shown in Fig. 1 b and 2 a. Some significant differences became evident when the measured orientation topographies were compared. In the alloy matrix deformed to 75 %, the distances between the high angle grain boundaries (HAGB) in the normal direction (ND) to the sheet plane were typically smaller than 1 μm, as shown in Fig. 2 c. In the pure metal, the thickness of similarly oriented layers often exceeded 10 μm, even for the deformation of 90 %, as shown in Fig. 1 a, c. These layers were composed of parallel bands or clusters of subgrains that were strongly elongated in the RD. In some of them, relatively small but accumulating disorientation angles[1] occurred (Fig. 1c). Because of this accumulation, large disorientation angles (up to ~ 20 °) between the first and the last subgrain in the band occurred frequently. Orientation changes of this type are characteristic for transition bands (Dillamore et al., 1972). The alternation of orientation patterns was also recognized. The high frequency of the low angle grain boundaries (LAGB) inside the band indicates a well-developed subgrain structure. With no further analysis of the pure metal deformation microstructure, we can only conclude that it consists of thick deformation and transition bands, and the density of HAGBs in the ND is low.

The crystallographic orientation characteristics of the alloy were quite different from those of the pure metal. The matrix consisted of well-developed HAGBs. The distances between them along ND were much smaller than those in the pure metal and never exceed a few hundreds of nanometers. LAGBs in the elongated thin matrix grains were less ordered and created a less-expanded subgrain structure. In the laminar microstructure of the alloy, small (<<1 μm) and large (1÷3 μm) precipitate particles of the second phase were scattered. Around the large particles, zones of localized strain were identified. These deformation zones consisted of

[1]A given misorientation can be described by a rotation axis and an angle of rotation. For a material with crystal symmetry, there is more than one angle of rotation. The angle with the absolute value smallest of all possible angles of rotation is called the disorientation angle.

ultrafine (50 – 200 nm) grains and more or less bent microbands of the matrix (Fig. 3 b, 4 b). The orientation image of the alloy clearly suggests that microstructural evolution occurs by grain subdivision at a very small scale compared to the original grain size, which was approximately 100 μm in this case. This result is presented in Fig. 2 c and 3 d, showing large orientation variations over a region as small as a few micrometers. Such rapid changes in orientation may demonstrate that volumes characterized by a combination of slip systems can be very small.

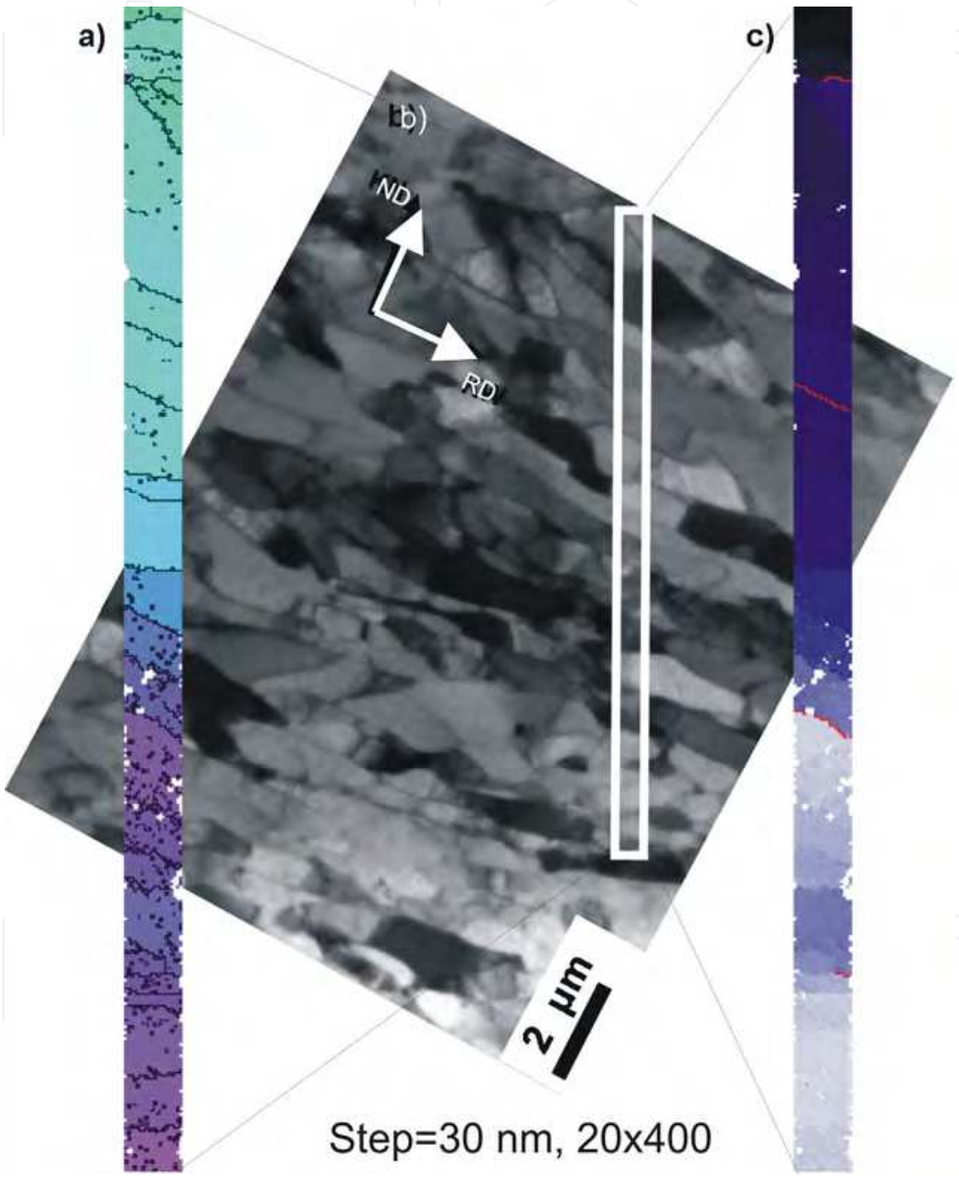

Fig. 1. As-deformed microstucture of 90% cold-rolled aluminum, the TEM bright field image (b) and orientation topographies (a and c). On the map (c) the color change indicates a deviation from the initial orientation (dark blue) to the disoriented orientation (light blue); black lines (a) - low angle grain boundaries (>1 °), red lines (c) - the boundaries with a disorientation angle > 5 °; the points where the diffraction pattern has not been solved are shown in white.

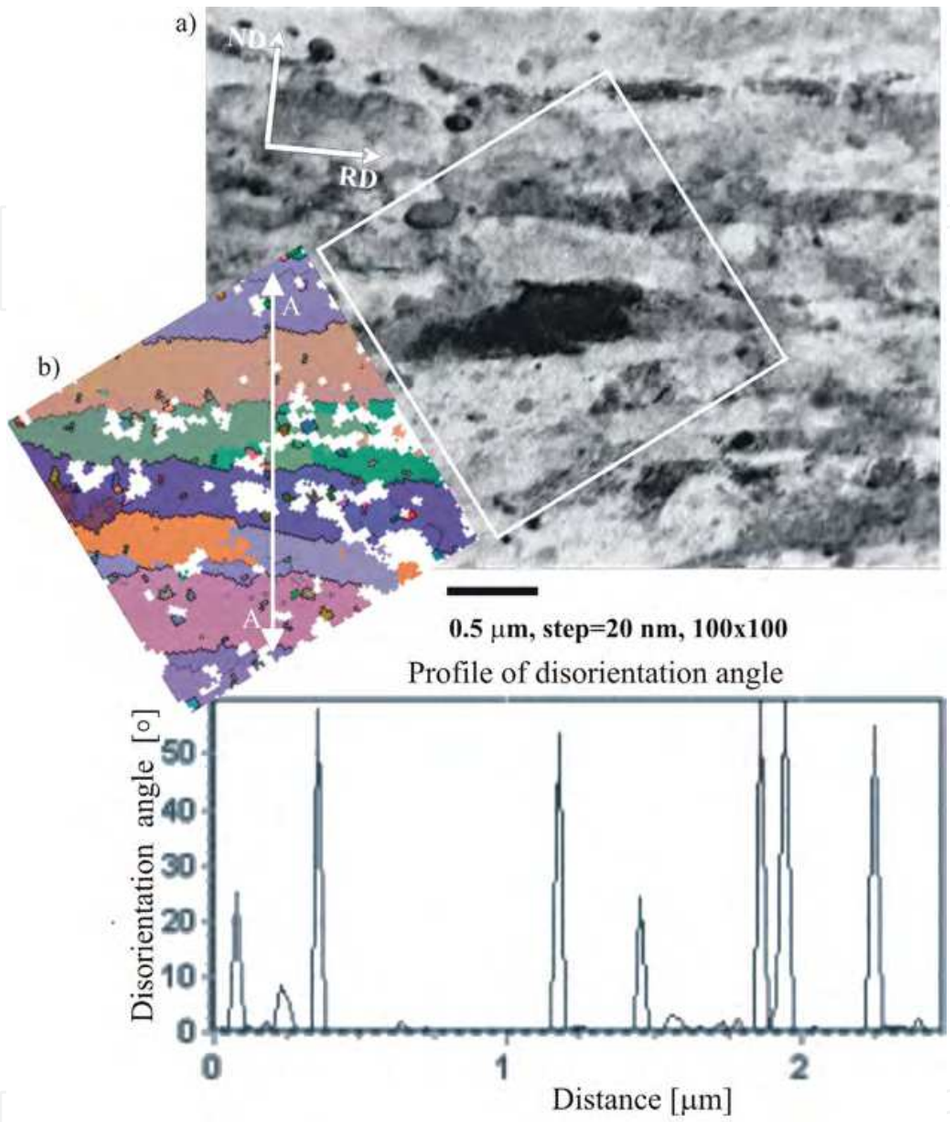

Fig. 2. a) As-deformed microstucture of 75% cold-rolled 6013 alloy, longitudinal section, TEM. b) Orientation topography of the matrix area, black lines show high angle grain boundaries; white regions are not indexed. c) Disorientation angle profile along A-A line (b), (Sztwiertnia et al., 2007).

The global crystallographic textures of both materials were similar and corresponded to the well-known rolling texture of FCC metals with high stacking fault energies (such as pure aluminum). Such a texture is characterized by the concentration of components along two orientation fibers. The main one, called the α fiber, runs diagonally through the orientation space containing the preferred texture components S {123}<634> and Cu {112}<111>. The other one, called the β fiber, includes Goss {011}<100> and Bs {011}<211> components (Sztwiertnia et al., 2005).

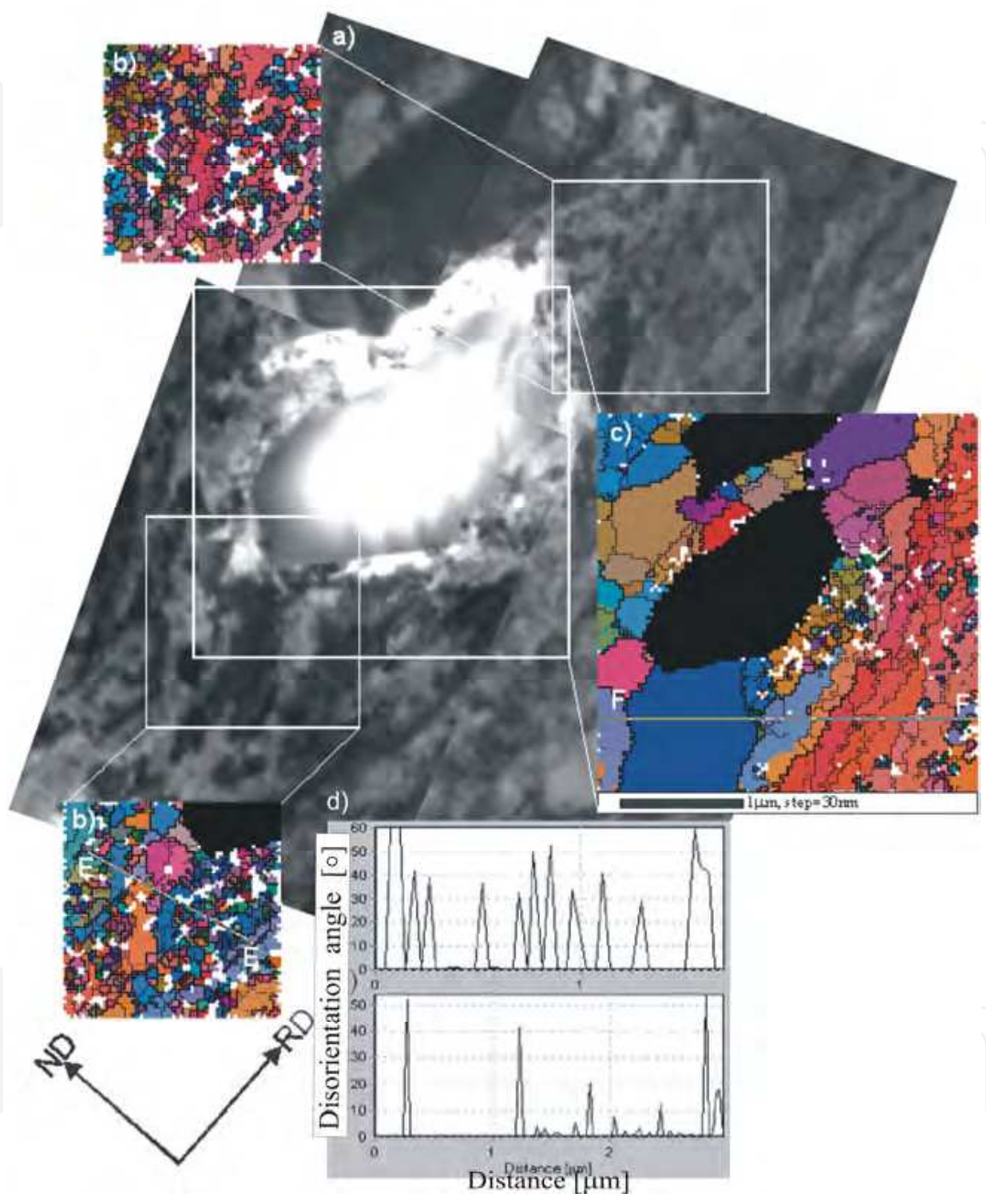

Fig. 3. a) As-deformed microstucture of 75% cold-rolled 6013 alloy, the deformation zone around the large particle, longitudinal section, TEM. Orientation topographies in areas of the deformation zone before (b) and after (c) heating *in situ* in TEM; particles of the second phase are shown in black, white regions are not indexed; thick lines indicate high angle grain boundaries, thin lines indicate low angles grain boundaries. d) Examples of disorientation angle profiles along E-E and F-F (Sztwiertnia et al., 2007).

2.3 Microstructure changes during annealing

The cold-rolled alloy was tested using the non-isothermal annealing method in a differential calorimeter. On the basis of these tests, as well as the microscopic analysis of the microstructures of the appropriately annealed samples, it was possible to state that the two separate peaks of the stored energy release correspond to the two stages of the recrystallization process (Fig. 6 a).

The *in situ* tests in the TEM allowed the determination of the sequence of events occurring at the beginning of recrystallization in the deformation zones around the large particles and in the matrix beyond those areas. First, the deformation microstructure was carefully examined. In the deformation zones around the large second phase particles, small grains and distorted fragments of microbands were identified. The small grains were approximately 50-200 nm in size. The strong orientation changes, greater than 15°, either identify HAGBs lying at distances lower than 200 nm or they are an effect of strong grain bending, as shown in Fig. 3 b, 4 b. To precisely distinguish between these two phenomena, small-step orientation maps were generated. The broad distribution of orientations in the deformation zones tended to group in the range of the deformation components after rotation around the transverse (TD) or the normal direction (ND) to the sheet plane (Sztwiertnia et al., 2005). This type of rotations suggests that at least a part of the strong orientation changes may be a result of the accumulation of small disorientations along a bent grain. In the matrix outside of the DZs, the HAGBs lie roughly parallel to the sheet plane at distances of 0.5 - 1 μm along the ND (Fig. 2 b).

After the sample was annealed in the microscope, the same areas as in the deformation state were investigated. Figures 3 c and 4 c show examples of DZ orientation maps after *in situ* annealing. Nuclei and new grains appeared in the vicinity of the deformation zone. The orientations of crystallites in the deformed state commonly lay in the area of a particular new grain or nucleus (Fig. 4 d, e). For each orientation of a new grain, at least one similarly oriented fragment of the deformed matrix was found. Some of the nuclei were growing within the zone defined by the migration of HAGBs, a result that was confirmed by a significant reduction of their density in those zones after annealing to the temperature of the first peak (Fig. 3 c, d and 4 b, c). The shape of some new grains suggests that they could have been formed as a result of the local recovery of strongly bent fragments of matrix microbands, as shown in Fig 4 c.

Partial misorientation distribution functions (PMDF) were calculated between the grains in the deformed state and the new grains that appeared at the same location (Fig. 5). PMDFs for both the 75 and 90 % deformed materials show a random distribution of misorientations. This distribution suggests that there was no special orientation relationship describing favored growth.

In the deformation zones at very early stages of the recrystallization, broad-spectrum HAGBs appear to have been active and mobile. At that time, no migration of HAGBs in the matrix areas outside the zones was observed.

To examine the significance of the *in situ* experiments, the microstructures of TEM-annealed thin foils were compared with the microstructures of thin foils prepared from bulk samples heated in a calorimeter to obtain a specified recrystallization stage. The comparison shows

that the processes occurring in the thin foils and in the bulk samples were, at least qualitatively, the same. The temperature range of the first recrystallization peak was found to produce nucleation, which is accompanied by some limited enlargement of new grains in the sheet plane.

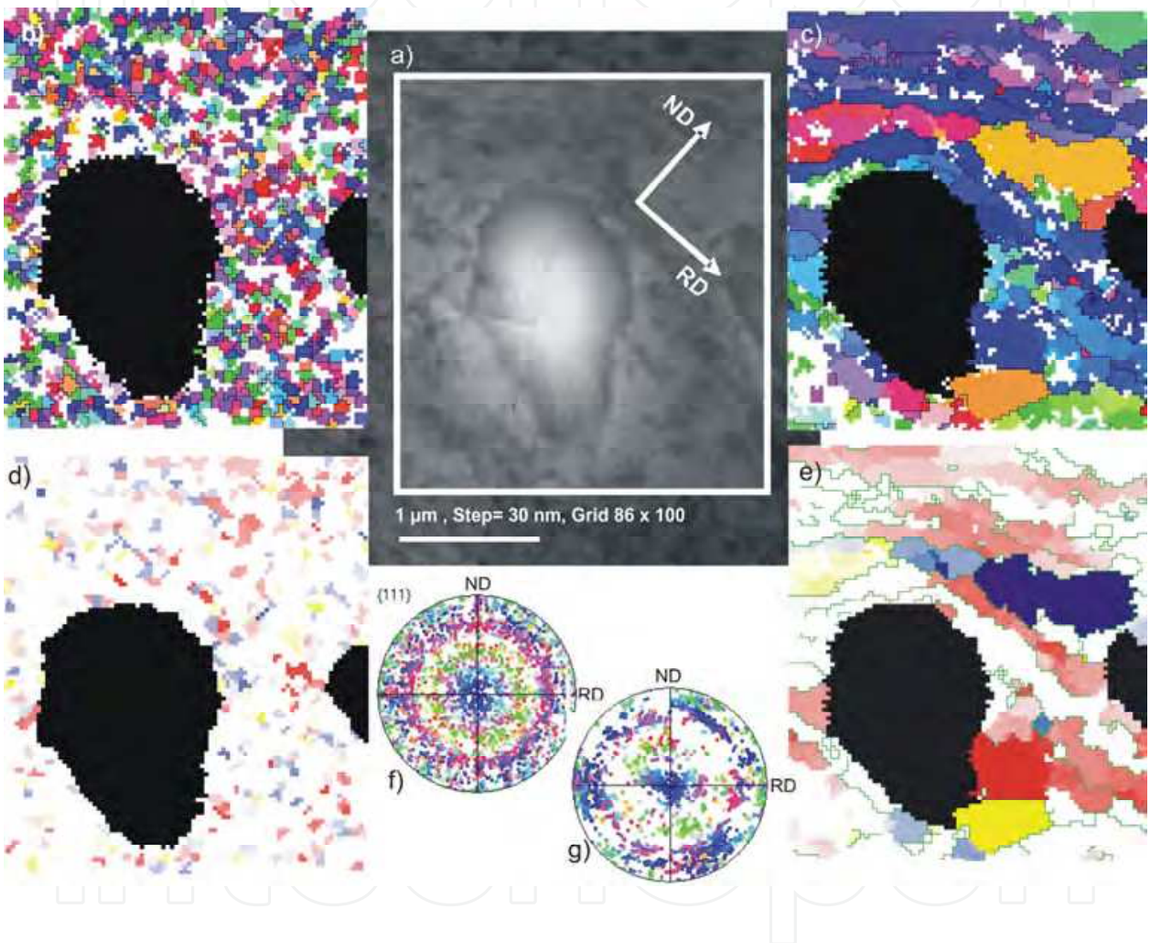

Fig. 4. a) Microstructure of 6013 aluminum alloy cold rolled to 90%, the deformation zone surrounding a large particle (a), longitudinal section, TEM. Orientation topographies and pole figures in areas of the deformation zone before (b, f) and after (c, g) heating *in situ* in TEM; particles of the second phase are shown in black, white regions are not indexed; thick lines indicate high angle grain boundaries, thin lines indicate low angle grain boundaries. Areas of similar orientations (blue, red, yellow) before and after annealing (d, e) (Bieda et al., 2010).

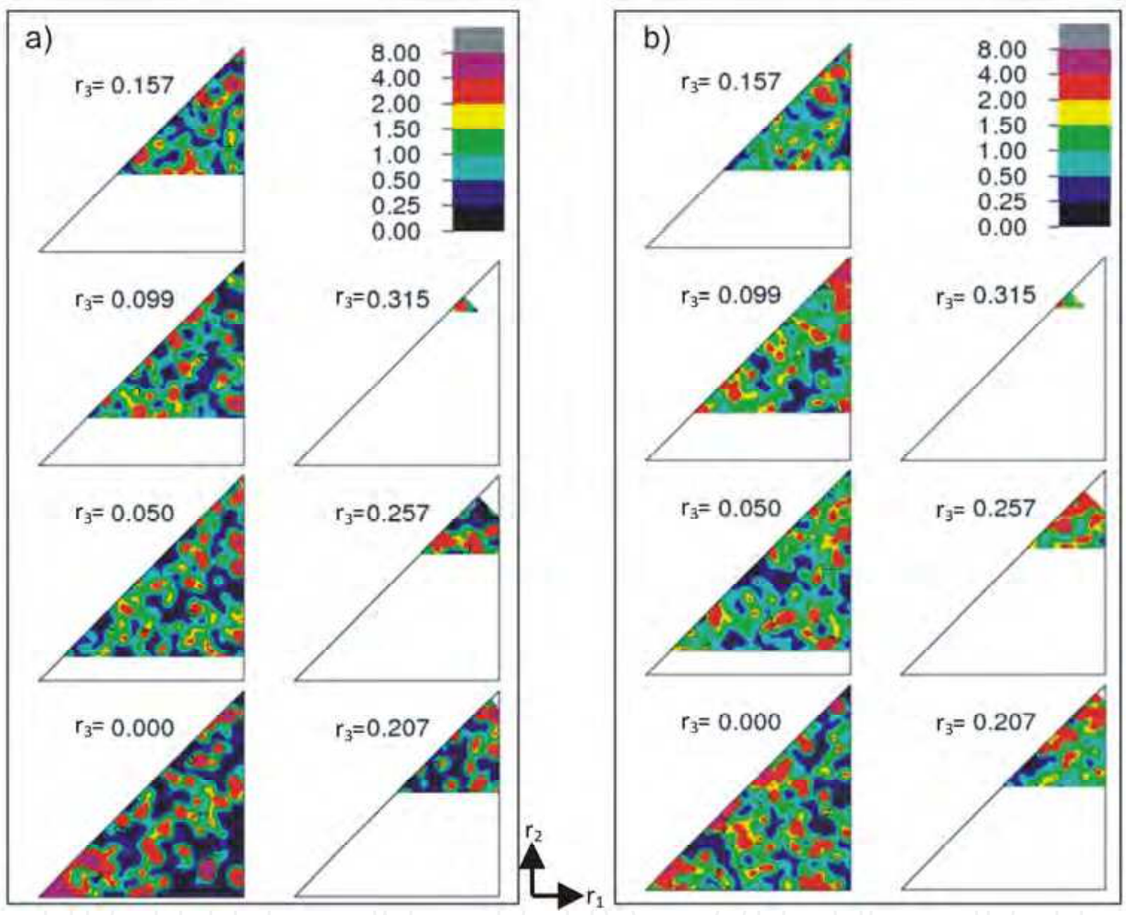

Fig. 5. Partial misorientation distribution functions showing the orientation relationships between the crystallites from the deformation zones (before annealing) and the new grains appearing in their positions after annealing (a) 75% cold-rolled 6013 aluminum alloy, (b) 90% cold-rolled 6013 aluminum alloy; Rodrigues' representation r_1, r_2, r_3, cross-section r_3=const., asymmetric domain (O, O) (Bieda et al., 2010).

By way of example, Fig. 6 c shows the orientation topography in the 75 % cold-rolled sample that was heated to 330 °C in a calorimeter. The appearance of new grains with sizes up to a few micrometers can be observed around the large particle. These new grains, similar to those in the *in situ* experiment, were formed as a result of nucleation and the consequent growth of nuclei inside the zone. At the examined temperature, the arrangement of LAGBs can also be observed in the elongated grains of the matrix outside the zone. The annihilation of these boundaries takes place at higher temperatures, near the end of the first peak.

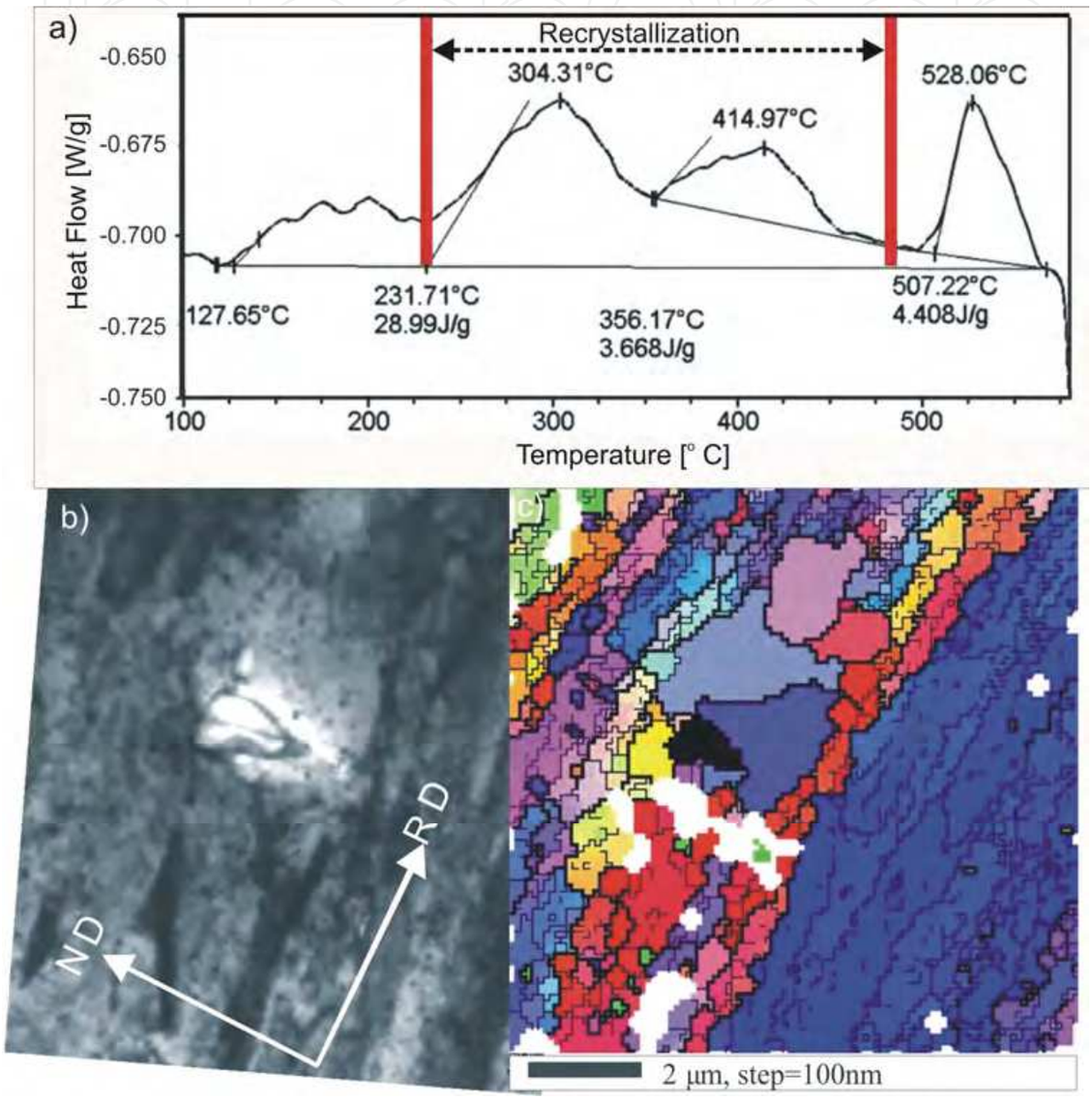

Fig. 6. a) Power differences, representing the release of stored energy from 75 % cold-rolled 6013 aluminum alloy as a function of annealing temperature. b, c) As-deformed microstructure and orientation topography of 6013 aluminum alloy 75 % cold-rolled and subsequently heated in the calorimeter to 330 °C: particles of the second phase are shown in black, white regions are not indexed; thick lines indicate high angle grain boundaries, thin lines indicate low angle grain boundaries; TEM, (Sztwiertnia et al., 2007).

The phenomenon of the annihilation of LAGBs and the growth of new grains in the sheet plane (mainly, parallel to the RD) was also observed in the SEM results (Fig. 7). The SEM measurements of the orientation topographies were made on samples heated to appropriate temperatures from the range of the first peak (Fig. 5 a). These observations fully confirm the TEM results and show that after the recrystallization of the deformation zones, local recovery processes (coalescence of subgrains) take place in the matrix. These local recovery processes lead to the annihilation of the LAGBs between chains of subgrains lying parallel to the sheet plane and, consequently, to the production of long grains with a low density of lattice defects. The growth of the elongated grains in the ND occurs rarely or not at all within the temperature range of the first peak. The migration of HAGBs in the matrix becomes the main process within the temperature range of the second peak. Heating of the sample to the temperature of the end of this peak leads to the complete discontinuous recrystallization of the material (Fig. 7 c). The recrystallized microstructure is dominated by elongated grains (up to 30 μm in length along the RD). It also includes groups of smaller grains, which are often almost equiaxial. After the discontinuous recrystallization, the grains are a few times thicker than they are in the state observed at the end of the first stage.

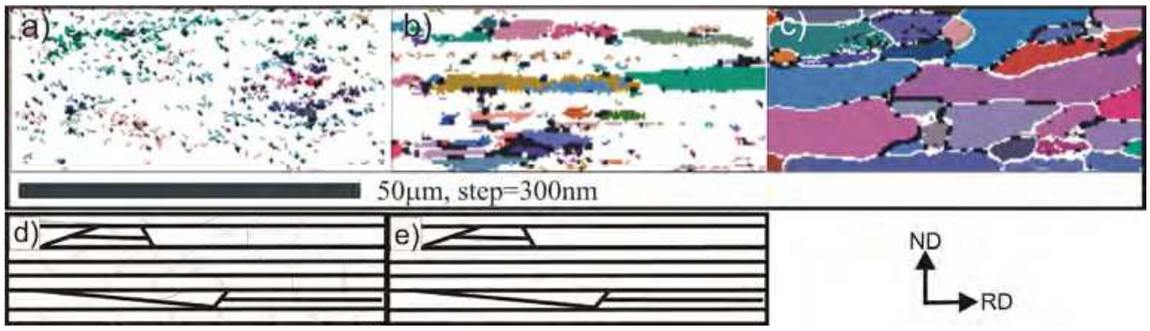

Fig. 7. Orientation topographies of recrystallized grains in 6013 aluminum alloy 75% cold rolled and subsequently heated in the calorimeter to: (a) 330 °C, (b) 350 °C and (c) 480 °C, regions of unsolved diffraction (approximately corresponding to the deformed areas) are shown in white, EBSD/SEM/FEG. d) and e) Schematic representation of the deformed microstructure before and after annealing to the temperatures from the end of the first recrystallization peak, Fig. 2; thick lines indicate high angle grain boundaries, thin lines indicate low angle grain boundaries.

3. Summary

Orientation topography provides basic local and global information about microstructures by allowing the identification and description of occurring regularities. The OM technique in TEM is a useful tool for the quantitative and qualitative characterization of fine crystalline and deformed microstructures in polycrystalline materials. It is possible to obtain information about grain distribution, misorientation between grains, material phases, the local orientation distribution function, and the misorientation distribution function. Replacement of the SEM measurements by TEM measurements improves the spatial resolution to a few nanometers. Both SEM and TEM can be used for complementary analysis of crystalline materials at the ”micro” and “nano” scale, respectively. Together with *in situ* studies, orientation mapping in TEM can provide additional information about the behavior

of a material during annealing, particularly in zones of greater deformation. The example of orientation characteristics presented in this chapter illustrates only some aspects of the applicability of these techniques. Orientation mapping in a transmission electron microscope was successfully applied to the study of microstructural changes during the initial stage of recrystallization in an aluminum alloy with a bimodal second-phase particle distribution. The images of the microstructure in the representative areas of a sample of deformed aluminum alloy 6013, described by measurements of orientation topography, shows greatly advanced grain fragmentation.

In situ investigations in TEM, calorimetric measurements, and orientation mapping in TEM and SEM demonstrate that the recrystallization of the tested material can be considered to occur as a number of partly overlapping processes that proceed in two stages. These stages correspond to the two separate stored energy release peaks. In the initial stage, the deformation zones around large second phase particles act as sites for particle-stimulated nucleation. This nucleation is accompanied by the growth of nuclei. However, the migration of high angle grain boundaries only occurs in deformation zones. At the same range of temperatures, some enlargement of new grains in the matrix (outside of the deformation zones) was also observed. The formation of grains elongated primarily in the direction parallel to the rolling direction may be correlated to the processes of local recovery, which is triggered in the deformation zones. Grain elongation then continues to develop along the bands of the deformed matrix in the directions of low orientation gradients. The elongated grains appear because of the annihilation of low angle grain boundaries between chains of subgrains lying in layers parallel to the sheet plane. As a consequence, new grains often have a plate-like character, with their shorter axis parallel to the sheet plane normal direction. Their lengths along the rolling direction may exceed 50 μm, while their thickness corresponds approximately to the distance between high angle grain boundaries in the normal direction outside the deformation zones; this dimension was not observed to exceed a few micrometers. In the second stage, high angle grain boundaries were observed to migrate in the direction of the high orientation gradient. This migration, mostly in the normal direction, was limited to "free areas" of the deformed matrix between bands of new grain formation in the initial stage of recrystallization.

4. References

Adams B.L., Dingley D.J (1994), *Orientation Imaging Microscopy: New Possibilities for Microstructural Investigations using Automated BKD Analysis*, Mater. Sci. Forum, 157-62 31.

Ardakani M.G., Humphreys F.J. (1994), *The annealing behavior of deformed particle-containing aluminum single crystals.* Acta Metal. Mater., 42, 763.

Bailey J.E. (1960), *Electron microscope observations on the annealing process occurring in cold-worked silver,* Phil. Mag., 5, 833.

Bieda M.,.Sztwiertnia K, Korneva A., Czeppe T., Orlicki R. (2010), *Orientation mapping study on the inhomogeneous microstructure evolution during annealing of 6013 aluminum alloy*, Solid State Phenom, 16, 13.

Bieda-Niemiec M. (2007), *Opracowanie systemu do automatycznego pomiaru map orientacji w transmisyjnym mikroskopie elektronowym do analizy mikrostruktury drobnoziarnistych materiałów metalicznych*, Thesis, Kraków IMIM PAN, in polish.

Dillamore I.L., Morris P.L., Smith C.J.F., Hutchinson W.B. (1972), *Transition Bands and Recrystallization in Metals,* Proc. Roy. Soc., 329A, 405.

Dingley D.J. (1984), *On-line determination of crystal orientation and texture determination in SEM*, Proc. Roy. Microsc. Soc., 19, 74.

Dingley D.J. (2006), *Orientation Imaging Microscopy for the Transmission Electron Microscope*, Mikrochim. Acta, 155, 19.

Haessner, F., Pospiech, J. and Sztwiertnia, K. (1983), *Spatial arrangement of orientations in rolled copper*, Mat. Sci. Eng.1, 1.

HKL (2007) http://www.oxford-instruments.com

Hu H. (1963), *Electron Microscopy and Strength of Crystals,* Interscience, London, 564.

Humphreys F.J. and Hatherly M. (2002), *Recrystallization and Related Annealing Phenomena*, Pergamon Press, Oxford.

Hutchinson W.B., Ray R.K. (1973), *On the feasibility of in situ observations of recrystallization in the high voltage microscope,* Phil. Mag., 28, 953.

Morawiec A. (1999), *Automatic orientation determination from Kikuchi patterns,* J. Appl. Cryst. 32, 788.

Morawiec A. (2004), *Orientations and Rotations. Computations in Crystallographic Textures.* Berlin, Heidelberg, New York: Springer-Verlag.

Morawiec A., Fundenberger J.J., Bouzy E., Lecomte J.S. (2002), *EP-a program for determination of crystallite orientations from TEM Kikuchi and CBED diffraction patterns"* J. Appl. Cryst., 35, 287.

Pospiech J., Lücke K. and Sztwiertnia K. (1993), *Orientation Distribution and Orientation Correlation Functions for Description of Microstructures*, Acta Metall. Mater. , 41, 305.

Rauch E.F., Dupuy L. (2005), *Rapid spot diffraction patterns identification through template matching*, Arch. Metall. Mater., 50, 87.

Roberts W., Lehtinen B. (1972), *On the feasibility of in situ observations of recrystallization in the high voltage electron microscope,* Phil. Mag., 26, 1153.

Schwartz A.J., Kumar M.,. Adams B.L, Field D.P. (2009), *Electron Backscatter Diffraction in Materials Science*, ISBN 978-0-387 88135-2, Springer.

Sztwiertnia K. (2008), *On recrystallization texture formation in polycrystalline fcc alloys with low stacking fault energies*, Int. J. Mater. Res., 99, 178.

Sztwiertnia K., Bieda M., Korneva A., Sawina G. (2007), *Inhomogeneous microstructural evolution during the annealing of 6013 aluminium alloy*, Inżynieria Materiałowa, Vol. 3 XXVIII, 476.

Sztwiertnia K., Bieda M., Sawina G. (2006), *Determination of crystallite orientations using TEM. Examples of measurements,* Arch. Metall. Mater. , 51, 55.

Sztwiertnia K., Haessner F. (1994), *In situ observations of the initial stage of recrystallization of highly rolled phosphous copper,* Mater. Sci. Forum, 157-162, 1069.

Sztwiertnia K., Morgiel J., Bouzy E. (2005), *Deformation Zones and their Behaviour during Annealing in 6013 Aluminim Alloy,* Arch. Metall. Mater. 50, 119.

TSL (2007) http://www.edax.com

Wright S.I., Adams B.L. (1992), *Automatic analysis of electron backscatter diffraction patterns*, Met. Trans. A 23, 759.

Zaefferer S, Baudin T, Penelle R (2001), *A study on the formation mechanisms of the cube recrystallization texture in cold rolled Fe-36% Ni*, Acta Mater. , 49, 1105.

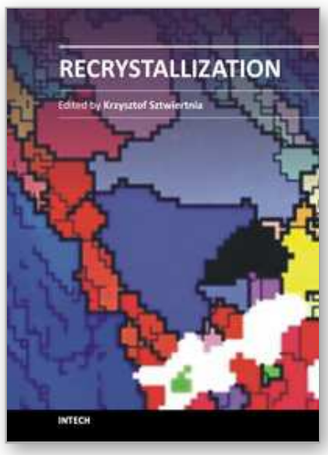

Recrystallization

Edited by Prof. Krzysztof Sztwiertnia

ISBN 978-953-51-0122-2
Hard cover, 464 pages
Publisher InTech
Published online 07, March, 2012
Published in print edition March, 2012

Recrystallization shows selected results obtained during the last few years by scientists who work on recrystallization-related issues. These scientists offer their knowledge from the perspective of a range of scientific disciplines, such as geology and metallurgy. The authors emphasize that the progress in this particular field of science is possible today thanks to the coordinated action of many research groups that work in materials science, chemistry, physics, geology, and other sciences. Thus, it is possible to perform a comprehensive analysis of the scientific problem. The analysis starts from the selection of appropriate techniques and methods of characterization. It is then combined with the development of new tools in diagnostics, and it ends with modeling of phenomena.

How to reference

In order to correctly reference this scholarly work, feel free to copy and paste the following:

K. Sztwiertnia, M. Bieda and A. Kornewa (2012). Application of Orientation Mapping in TEM and SEM for Study of Microstructural Evolution During Annealing – Example: Aluminum Alloy with Bimodal Particle Distribution, Recrystallization, Prof. Krzysztof Sztwiertnia (Ed.), ISBN: 978-953-51-0122-2, InTech, Available from: http://www.intechopen.com/books/recrystallization/application-of-orientation-mapping-in-tem-and-sem-for-study-of-microstructural-evolution-during-anne

INTECH
open science | open minds

InTech Europe
University Campus STeP Ri
Slavka Krautzeka 83/A
51000 Rijeka, Croatia
Phone: +385 (51) 770 447
Fax: +385 (51) 686 166
www.intechopen.com

InTech China
Unit 405, Office Block, Hotel Equatorial Shanghai
No.65, Yan An Road (West), Shanghai, 200040, China
中国上海市延安西路65号上海国际贵都大饭店办公楼405单元
Phone: +86-21-62489820
Fax: +86-21-62489821

IntechOpen